

# Macroporous silicon deep UV filters.

Vladimir Kochergin<sup>\*1</sup>, Ofer Sneh<sup>2</sup>, Mahavir Sanghavi<sup>1</sup>, Philip R. Swinehart<sup>1</sup>

<sup>1</sup>Lake Shore Cryotronics, Inc., 575 McCorkle Blvd., Westerville, OH, 43082

<sup>2</sup>Sundew Technologies, LLC, 1619 Garnet St., Broomfield, CO 80020

**Abstract-** A novel method to make deep and far UV optical filters from macroporous silicon is presented. This type of filter consists of an array of parallel, independent, leaky waveguides made in the form of a free-standing, two-dimensionally ordered silicon structure with pore walls coated by a dielectric multilayer. This structure offers high levels of rejection within a very wide rejection band combined with a high level of transmission within a pass band that could be centered anywhere in the deep and far UV range. In addition, unlike common interference-based filters, the spectral position of the pass and rejection bands is independent of the angle of incidence. These filters consist of two-dimensionally ordered Macroporous Silicon (MPSi), fabricated by electrochemical etching of silicon wafers. Multilayer coating of the pore walls results in the band-pass, short-pass, or band-blocking transmittance spectra of MPSi filters. The Atomic Layer Deposition (ALD) technique is used for such purposes because of its unique ability to conformally coat very high aspect ratio structures. It is demonstrated that ALD is capable of coating high aspect ratio pores and also permits the “engineering” of the optical properties of individual layers by creating a nanolattice of different materials on the pore walls.

## I. INTRODUCTION

The majority of currently available UV filters are based on interference in multilayer stacks (interference filters). These filters have a number of drawbacks. The main problem usually is the insufficient width of the rejection band that can be achieved at a reasonable cost. In addition, in the deep UV spectral range, there are few materials sufficiently transparent below 250 nm. Further, many of these material combinations provide low refractive index contrast and/or are not environmentally stable, having poor adhesion or susceptibility to moisture. Multilayers incorporating these materials are thus subject to delamination and wavelength drift when exposed to humid atmospheres. This in turn causes many problems for the end users, who must continuously worry about controlling the environments in their equipment. Low refractive index contrast between adjacent layers causes other problems for applications in terms of more layers required, thus higher cost and lower robustness. Another conventional approach is filtering by a number of reflective diffraction gratings, which provides fairly good filtering, but at the cost of large and heavy structures, requiring tight alignment.

Another design of UV filters was recently proposed [1-2]. In these filters, the waveguiding in the pores becomes the key phenomenon that determines the light transmission. The waveguides, with cores formed by the pores in MPSi, are essentially leaky as long as light can penetrate into a higher index cladding. The filtering is provided by the wavelength-dependent optical losses. A similar filtering

mechanism in the far infrared spectral range ( $\lambda > 100\mu\text{m}$ ) has been reported for leaky waveguide arrays in narrow holes drilled in a metal sheet [3-4]. Previously, the proof of principle of operation of such a filter was demonstrated with single-layer pore wall coating (achieved by means of thermal oxidation of the MPSi layer) [2] and with a five layer pore wall coating deposited by Low Pressure Chemical Vapor Deposition technique (LPCVD) [5]. The drawback of LPCVD is the narrow choice of pore coating materials and difficulty in achieving the required uniformity of the coating across the high aspect ratio structures. In this paper, a feasibility study of ALD deposition of dielectric multilayer into the pores is reported.

## II. FILTERING MECHANISM IN MPSi UV FILTERS

As has been previously shown [1-2], at wavelengths below  $\sim 1\mu\text{m}$  a free-standing (meaning with pores opened on both ends) MPSi layer can be considered as an array of leaky waveguides. Light travels through the leaky waveguides by reflecting from their walls. The optical losses associated with non-total reflection from the walls define the transparency range of the layer. The optical loss coefficient is a function of pore size, geometrical pore distribution, pore wall coating structure and wavelength. It also depends on the smoothness of the pore walls, uniformity of the pore cross-section and pore wall coating structure along the pore length.

A MPSi structure with uncoated pore walls shows well-pronounced short-pass filtering behavior, first reported in ref. [6]. However, in an uncoated MPSi layer, the sharpness of the rejection edge is closely related to the rejection edge spectral position. The sharpness of the rejection edge is a function of pore size and pore length. An increase in sharpness is possible only with a decrease of transmission in the pass band accompanied by a strong blue-shift of the rejection edge of the filter. As has been theoretically shown before [1-2], the sharpness of the spectral transmission characteristics of an MPSi filter can be substantially improved by applying thin film coatings to the pore walls. This may be done by depositing a multilayer coating inside the pores using ALD.

A diagrammatic view of an MPSi structure with pore walls covered by several layers of different transparent dielectric materials is shown in Fig. 1. Such a coating on the pore walls causes dramatic modification of the spectral dependence of the leaky waveguide mode loss coefficient. Various designs of the multilayer coatings on the pore walls can be considered, depending on the choice of materials, desirable filter specifications, etc. To provide optimal performance, the materials comprising a multilayer coating do not have to be transparent over the pass band, rejection band and rejection edge, which is quite beneficial for deep and far UV filters,

since a number of dielectric materials that are transparent only over a part of the deep and far UV range (e.g., titanium dioxide, silicon nitride, silicon dioxide) can be used for these spectral ranges.

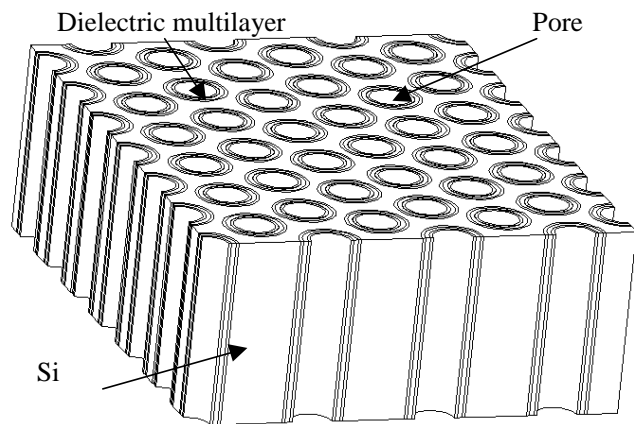


Fig. 1. Free-standing MPSi array with multiple layers of transparent dielectric materials uniformly covering the pore walls.

As an example, Fig. 2 gives the numerically calculated spectral dependence of the transmission through the MPSi membrane with five-layer pore wall coating. The pores were assumed to be  $350\text{ }\mu\text{m}$  deep and originally  $1.5\text{ }\mu\text{m}$  in diameter. In the calculations the dispersions of the real and imaginary parts of the refractive indices of silicon, silicon dioxide and silicon nitride were taken into account. One can see that while the silicon nitride absorption edge is located approximately at the  $290\text{ nm}$  wavelength, substantial transmission in the deep UV is possible.

One of the most attractive properties of the MPSi-based UV filters is the very strong level of rejection that is achievable. As follows from Fig. 2, the level of rejection can exceed 5 orders of magnitude over a very wide rejection range. The rejection edge sharpness and the rejection level are determined by both the number of layers on the pore walls and by the aspect ratio in the pores.

Tuning of the wavelength position of the pass band can be done by varying the structure of the multilayer coating, just as it can for common planar multilayer dielectric high-reflectance coatings. However, the tuning of the pass-band position for an MPSi structure is a considerably more complex task than the tuning the same tuning with ordinary multilayer filters. The shift of the position of the leaky waveguide mode propagation loss minimum may be accompanied by the reshaping of the whole mode propagation loss spectral dependence. To avoid this, one needs to take into account not only the structure of the multilayer coating on the pore walls, but also the pore parameters [2] (shape and cross-section).

It should be noted that besides the short-pass type of filter, it is possible to fabricate a band-pass filter based on coated MPSi layers as well. The peculiarity of the MPSi filter structure are such that, in order to exhibit narrow bandpass behavior, the coating on the pore walls should act as a narrow band reflector at an almost glancing angle of incidence (depending on a pore geometry at angles between  $80^\circ$  and  $86^\circ$ ). As it is well known, in order to form such a reflector one needs to use a substantial number of layers of materials with adequately close indices of refraction. This is because the width of

the band in this case is determined by the index contrast--the higher the contrast, the wider the band. This calls for the "engineering" of the refractive index of the layers in the multilayer stack, since the choice of transparent, environmentally stable and depositable materials is quite limited in the deep UV range. As will be shown later in this paper, the ALD technique is ideal for these purposes and the potential for multilayers of "engineered" materials will be experimentally demonstrated.

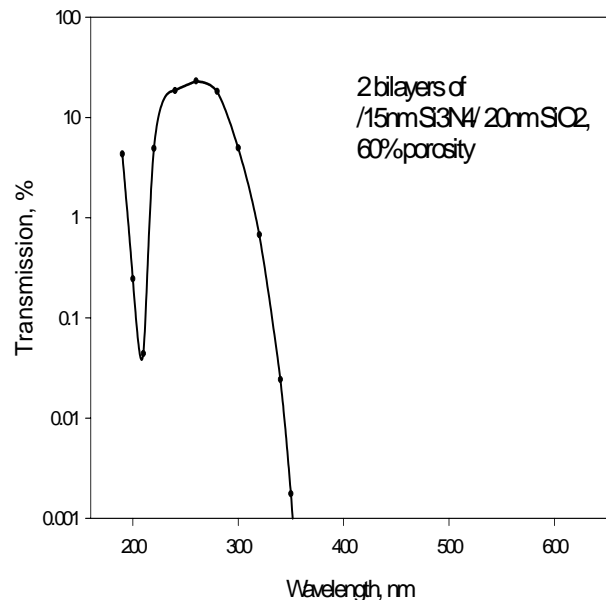
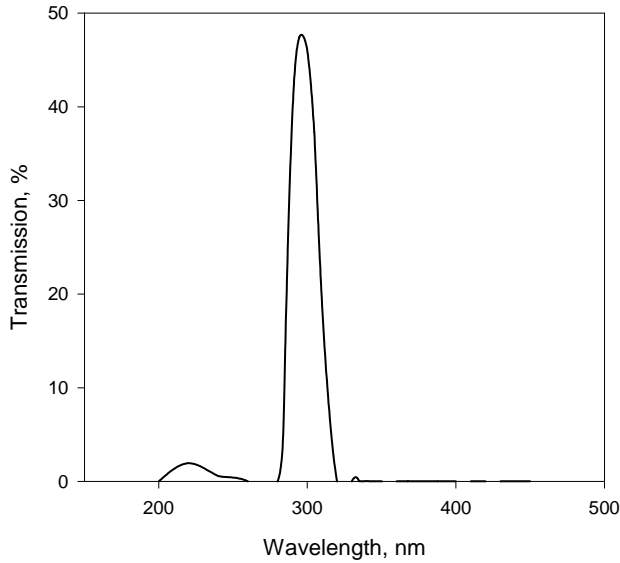


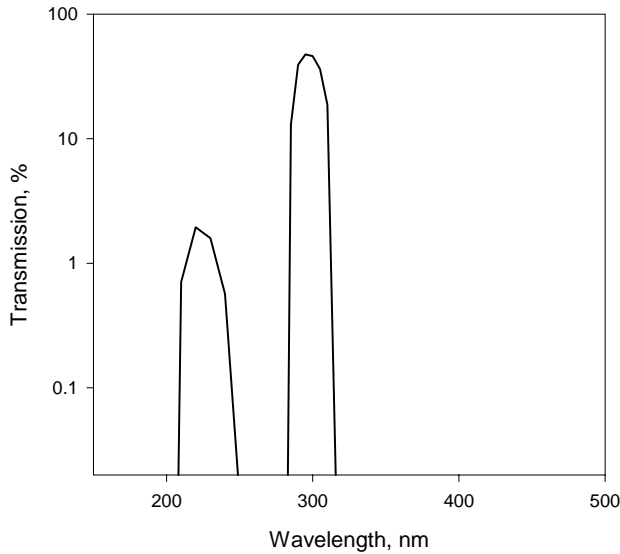
Fig. 2. Numerically calculated spectral dependences of the transmission through an MPSi membrane with a five-layer pore wall coating. The transmission is given on a logarithmic scale.

As an example, Fig. 3 gives the numerically calculated spectral dependences of the transmission through an MPSi membrane with a 9.5-bilayer pore wall coating. It is designed as a narrow bandpass filter with band centered at  $300\text{ nm}$ . The transmission in Fig. 3a is plotted on a linear scale, while that in Fig. 3b is given on a logarithmic scale. In calculations, the refractive indices of the layers were assumed to be 1.75 and 1.9. The dispersion of the dielectric constants in the pore wall coating was neglected. Such refractive indices are close to those of an  $\text{Al}_2\text{O}_3$  and  $\text{Al}_2\text{O}_3/\text{TiO}_2$  nanolaminated stack, discussed later in this paper. In calculations an MPSi membrane with an aspect ratio of 150 was used (such an aspect ratio is well within limits of the technology). The narrow bandpass transmission of such a structure is clearly demonstrated.

One should note that in addition to a quite high level of transmission within a reasonably narrow band, such a structure should exhibit high levels of rejection at wavelengths above the center of the band. Theoretical calculations also show a parasitic transmission peak at  $\sim 220\text{ nm}$ . However, this peak should be strongly suppressed in reality, since this peak is located at wavelengths below the  $\text{TiO}_2$  absorption edge (i.e., the  $\text{TiO}_2$  portion of a multilayer will be opaque). It appears in the theoretical curves because the imaginary parts of the refractive indices of the pore wall coating layers were neglected in the calculations as discussed previously.



a)



b)

Fig. 3. Numerically calculated spectral dependences of the transmission through an MPSi membrane with a 19-layer pore wall coating designed as a narrow bandpass filter with band centered at 300nm. The transmission in a) is plotted on a linear scale, while in b) it is given on a logarithmic scale.

Another important feature of MPSi UV filters is the capability of achieving a virtually unlimited rejection band on the longer wavelength side. The MPSi layer itself (uncoated or coated with dielectric multilayer), in addition to the pass band in the UV, also shows pass-bands throughout the near IR and IR (starting from approximately 1100nm). This transmission band was explained [2] as an appearance of an additional channel of transmission through the MPSi array due to the transparency of Si in the IR. It has already been demonstrated [5] that it is possible to completely suppress the transmission through waveguide modes by covering the first, second or both surfaces of the MPSi structure by a thin (100-200nm) metal

film to prevent the light from either coupling into or out of the Si waveguides. More than four orders of magnitude suppression of IR transmission was demonstrated by coating both sides of the MPSi membrane by relatively thin (100nm) metal layer. It was also demonstrated that in the case of a directional deposition technique (such as magnetron sputtering) the influence of the metal coating on the UV transmission window is reasonably small.

### III. FABRICATION OF MPSi UV FILTERS

The fabrication of MPSi UV filters consists of two main parts: 1) fabrication of macroporous silicon base structure (membrane) and 2) dielectric multilayer pore wall coating with ALD technique.

#### A. Macroporous silicon membrane formation

Porous Silicon (PSi) is normally thought of as a system of voids with the silicon web forming a solid matrix. The sizes of pores (and conversely the Si matrix) can vary in the range from nanometers to hundreds of micrometers. Macroporous Si (MPSi) refers to PSi with pore sizes above 100 nm. MPSi is usually formed by the electrochemical etching of Si in a solution containing hydrofluoric acid (HF). The pore size, shape and depth (as well as ordering) can be well controlled [7]. A schematic design of the anodization chamber is given in Fig. 6. The porosity,  $p$  (the volume fraction of voids within the silicon layer) of an array of macropores is determined by the etching current density,  $J$ , according to  $p = J/J_{PS}$ , where  $J_{PS}$  is the critical current density at the pore tips [7].

The wafer doping level, current density, electrolyte composition, and illumination (for n-doped Si) are all crucial parameters in determining the pore structure. By careful adjustment of the process conditions, it is possible to fabricate ordered MPSi arrays with pore diameters in the range from 500nm to 10μm and aspect ratios as high as 250:1.

The MPSi structure, as formed on an initially smooth, bare silicon surface, does not provide any long-range order. The macropores in such structures are usually disposed quite randomly. As discussed above, ordered MPSi arrays are required for DUV filter applications. To fabricate ordered pore arrays, etch-pits are required as pore nucleation points. To create etch-pits, the silicon wafer must be photolithographically patterned and chemically etched in an anisotropic etchant, such as hot KOH, prior to anodization.

Etching of MPSi layers usually takes place in a special electrochemical etching cell, such as the cell commercially available through ET&AT, Kiel, Germany. The unit has complete computer control over the etching parameters and backside illumination option, and several novel bath-parameter feedback techniques are the subject of recent patent applications.

In order to make MPSi layers free-standing, the un-anodized part of the silicon wafer must be removed from the back side. This can be done by means of inductively-coupled reactive ion etching or through chemical etching in hot KOH or EDP (Ethylene Diamine Pyrocatechol). As an example, Fig. 4 gives an SEM image of a cleaved, free standing MPSi layer.

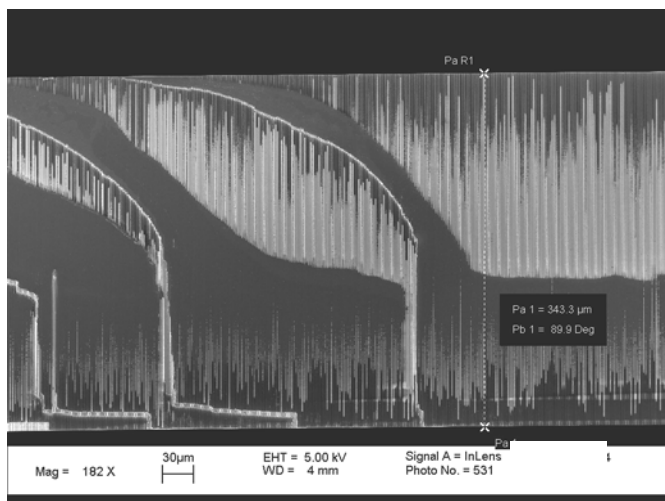


Fig. 4. SEM image of a cleaved free-standing MPSi membrane

### B. Atomic Layer Deposition Background

Atomic Layer Deposition (ALD) is a deposition technique that lays down films sequentially, one atomic layer after the other [8-10]. ALD films have unique pinhole-free and low stress properties that render them ideal candidates for many applications. The deposition process is performed with robust and atomic-level control of film thickness and properties without the need for in-situ monitoring. It deposits continuous and uniform films on any three-dimensional surface structure, penetrating the most narrow and deep grooves, vias and cavities.

ALD offers many advantages over other more conventional techniques and is best suited for some of the most challenging thin film deposition applications. ALD films can be uniquely grown continuously on substrates, avoiding the inferior, discontinuous transitions caused by nucleation [10]. As a result, ALD films grow pinhole-free and practically stress free. All other deposition techniques initiate film growth by nucleation.

ALD films have the proven ability to conformally coat the toughest three-dimensional structures. In addition, the layer-by-layer mechanism allows reproducible film engineering at the atomic level. Film engineering is key in enabling continuous growth of ALD films over a variety of substrates wherein typically the incompatibility of the film with the substrate is overcome by providing an ultrathin (several monolayers only) interface layer that is compatible with both the substrate and the film. Film engineering has also been proven to modify and improve film properties such as the suppression of the growth of disadvantageous polycrystalline films [8]. Amorphous films are an important property for narrow bandpass filter fabrication, as was assumed in the previous sections of this paper.

The recently introduced Synchronously-Modulated-Flow-Draw (SMFD) ALD equipment developed at Sundew Technologies, LLC, sets unprecedented milestones for ALD productivity [11], with factor improvements exceeding  $\times 16$  for wafer throughput per square foot,  $\times 50$  extended equipment uptime and  $\times 25$  extended vacuum pump lifetime. This breakthrough in productivity enables mass

production of ALD films in the film thickness range of  $\sim 1 \mu\text{m}$  and renders SMFD-ALD particularly suitable to many emerging ALD applications in semiconductor and non-semiconductor industries.

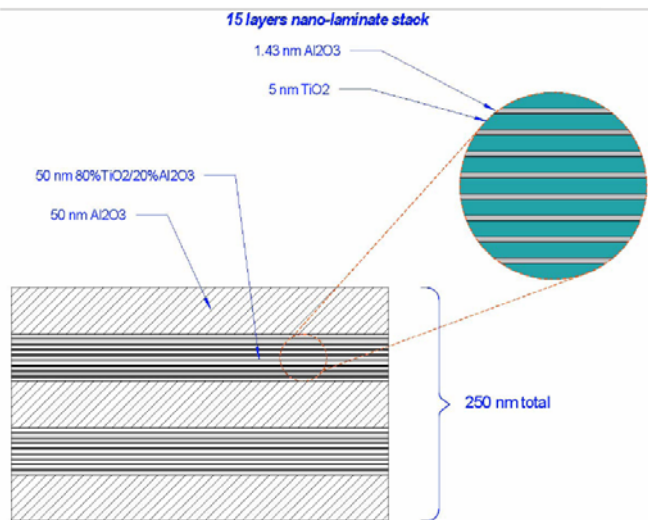


Fig. 5. Schematic cross-sectional drawing of the pore wall coating structure used in the experiment.

Macroporous silicon membranes are challenging due to the enhanced surface area of substrates. The actual area of a substrate with  $1.5 \times 1.5 \mu\text{m} \times \mu\text{m}$  opening and  $200 \mu\text{m}$  deep pores is enhanced by a factor of  $\sim \times 133$  in the case of 25% porosity. Accordingly, high-productivity ALD depends on the ability to deliver enormous chemical exposure within a short period of time and to utilize the chemicals effectively. For example, exposure delivery rates of  $\sim 2.5 \times 10^{20}$  molecules per second are essential for an ALD process with 95% chemical utilization efficiency over 150mm wafers. These rates and efficiency levels already have been demonstrated by Sundew Technologies for the deposition of  $\text{Al}_2\text{O}_3$  with an ALD enabling cycle time of  $< 0.5 \text{ sec}$ .

The motivation of this work was to demonstrate the capabilities of ALD technique on MPSi samples.

### C. Experimental demonstration of Atomic Layer Deposition of $\text{Al}_2\text{O}_3/\text{TiO}_2$ multilayer into the MPSi filter

A 250 nm thick ALD film stack was deposited over a MPSi sample using five, 50 nm thick alternating layers of  $\text{Al}_2\text{O}_3$  and alumina-titanate. The alumina-titanate layer comprises fifteen nanolaminated layers of 5.0 nm thick  $\text{TiO}_2$  and 1.43 nm thick  $\text{Al}_2\text{O}_3$  resulting in a 4:1  $\text{TiO}_2:\text{Al}_2\text{O}_3$  composition ratio that is sufficient to suppress the natural, disadvantageous agglomeration of  $\text{TiO}_2$  while achieving a relatively high optical index (see Fig. 5 for a schematic illustration of the layer-stack).

The  $300^\circ\text{C}$  process was implemented with precursor combinations of trimethylaluminum/ $\text{H}_2\text{O}$  for  $\text{Al}_2\text{O}_3$  and  $\text{TiCl}_4/\text{H}_2\text{O}$  for  $\text{TiO}_2$  with cycle times of 430 and 650msec, respectively. The resulting conformal coating is apparent in the SEM images of Fig. 6, indicating the feasibility of cost-effective, robust and reproducible multilayer growth over these challenging substrates and with the required conformality. The SEM clearly indicates that the 250 nm

layer stack is highly conformal. The high resolution SEM highlights the 5 layers stack, although sample charging effects blur the borders between the layers.

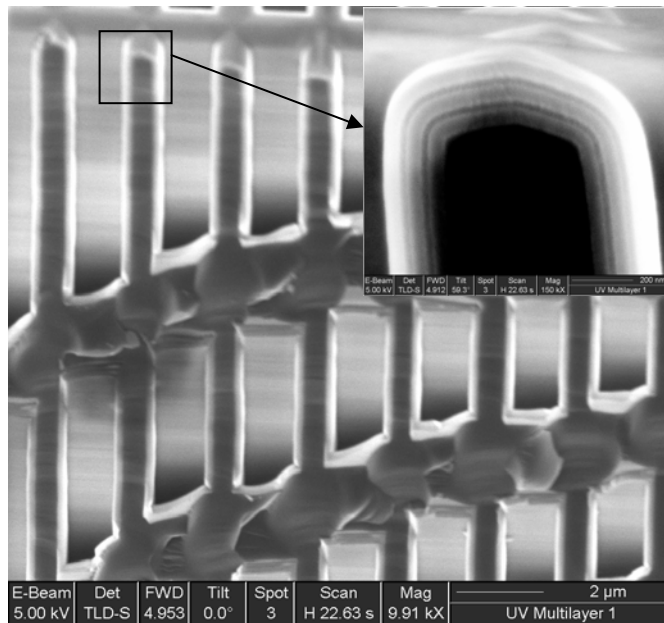


Fig. 6. Cross-sectional SEM images of an ALD-coated MPSi membrane with an  $\text{Al}_2\text{O}_3/\text{TiO}_2$  multilayer with the structure as in Fig. 4.

#### IV. CONCLUSIONS

In conclusion, we have demonstrated the feasibility of producing a new type of deep UV filter based on a porous silicon material. Short-pass, band-pass and even narrow-bandpass UV and deep UV filter designs have been shown. Complex multilayer pore wall coating by the ALD technique was successfully demonstrated. The possibility of depositing nano-engineered materials on the walls of MPSi to suppress otherwise disadvantageous island crystallization was experimentally indicated by the smoothness and uniformity of the coatings. Such filters are expected to find a wide range of applications in the deep UV spectral range where traditional approaches to filter design fail due to lack of suitable materials or other shortcomings.

#### ACKNOWLEDGMENTS

We want to thank the NASA SBIR program for funding this research under grant NNG05CA58C SBIR 2004-I, Deep Ultraviolet Macroporous Silicon Filters.

#### REFERENCES

- [1] I. Avrutsky and V. Kochergin, *Appl. Phys. Lett.*, **82**, 3590 (2003)
- [2] “*Omnidirectional Optical Filters*” Vladimir Kochergin, Kluwer Academic Publishers, Boston, ISBN 1-4020-7386-0 (2003)
- [3] F. Keilmann, *Int. J. Infrared and Millimeter Waves*, **2**, 259 (1981)
- [4] T. Timusk, P. L. Richards, *Appl. Optics*, **20**, 1355 (1981)
- [5] V. Kochergin, M. Christophersen, P.R. Swinehart, *Proc. SPIE Vol. 5554*, p. 223-234 (2004)
- [6] V. Lehmann, R. Stengl, H. Reisinger, R. Detemple, W. Theiss, *Appl. Phys. Lett.*, **78**, 589 (2001)
- [7] V. Lehmann, *J. Electrochem. Soc.* **140**, 2836 (1993)
- [8] M. Ritala and M. Leskela, in: H. S. Nalwa, (Ed), *Handbook of Thin Film Materials*, Academic Press, San Diego, 2001, Vol. 1, Chapter 2, p 103
- [9] S.M. George, A.W. Ott and J.W. Klaus, *J. Phys. Chem.* **100** (1996) 13121
- [10] O. Sneh, R.B. Clark-Phelps, A.R. Londergan, J.L. Winkler and T.E. Seidel, *Thin Solid Films*, **402/1-2** (2002) 248
- [11] O. Sneh, *Solid State Technology*, November 2003, p. 22

Patents awarded and pending